# Energy & Enviromental Science

## ARTICLE

# Fluorination on both D and A Unit in D−A Type conjugated copolymer based on difluorobithiophene and benzothiadiazole for high efficient polymer solar cells †

Jea Woong Jo,[a] Jae Woong Jung,[a] Eui Hyuk Jung,[a] Hyungju Ahn,[b] Tae Joo Shin,[b] and Won Ho Jo*[a]

Fluorination of conjugated polymers is one of effective strategies to tune the frontier energy levels for achieving high efficiency polymer solar cells. In this study, three fluorinated D−A polymers, consisting of 3,3'-difluoro-2,2'-bithiophene and 2,1,3-benzothiadiazole (BT) with different number of fluorine substitution, were synthesized in order to investigate the effect of fluorination on their photovoltaic properties. The polymers with fluorinated BT show lower frontier energy levels, improved polymer ordering, and narrower fibril size in the blend with $PC_{71}BM$. The polymer with mono-fluorinated BT exhibits a superior PCE of 9.14% due to high SCLC hole mobility, mixed orientation of polymer crystals in the active layer, and low bimolecular recombination. This result demonstrates that the fluorine content in conjugated polymer should be controlled for optimizing optoelectrical and photovoltaic properties of fluorinated conjugated polymers.

## Introduction

Over the past decade, polymer solar cells (PSCs) have intensively been investigated as a promising renewable energy source due to solution processability, rapid energy payback time and mechanical flexibility,[1] and understanding the relationship between chemical structure and optoelectrical properties of polymers largely contributes to such rapid development of high performance PSCs: high power conversion efficiencies (PCEs) of PSCs have been achieved by designing the chemical structure of conjugated polymer using the functional group substitution,[2] the fusion of aromatic rings,[3] the optimization of side chains,[4] and end-group modification.[5]

Among several strategies for designing conjugated polymers, the substitution of fluorine atom on conjugated polymer backbone has attracted much attention for the last few years due to their unique advantages including energy level lowering without sacrifice of bandgap, improvement of molecular ordering by induced dipole along C−F bond, and no steric hindrance due to small size of fluorine atom (van der Waals radius, r = 1.35 Å). Recently, it has been reported that the PSCs based on fluorinated conjugated polymers exhibit high PCEs over 7%.[6] Although fluorination on conjugated polymers has many benefits, the fluorination can also lead to negative effects on polymer properties such as low solubility in organic solvent, unsuitable energy levels for exciton separation and charge transport, and large aggregation of polymers in the active layer of PSCs.[7] Hence, the degree of fluorination on conjugated polymer (i.e., the number of substituted fluorine atom in one

repeating unit of the polymer) should be optimized for achieving high efficient PSCs.

Currently, conjugated polymers based on 3,3'-difluoro-2,2'-bithiophene have been proposed as promising candidates for high performance PSCs by our group: a polythiophene derivative, comprised of 3,3'-difluoro-2,2'-bithiophene and 3,4-dialkylthiophene, has shown a promising PCE of 5.2%.[8a] We have also reported synthesis and photovoltaic properties of two kinds of D−A polymers with each being fluorinated on D and A unit, where quaterthiophene and 2,1,3-benzothiadiazole (BT) are used as D and A unit, respectively, in order to investigate the effect of fluorination position on photophysical and photovoltaic properties of the polymers. Although the fluorination on either D or A unit effectively enhances intermolecular interaction and lowers both the lowest unoccupied molecular orbital (LUMO) and the highest occupied molecular orbital (HOMO) energy levels retaining a low bandgap of 1.58 eV, the polymer with fluorinated D unit exhibits a high PCE of 7.10% while the polymer with fluorinated A unit exhibits a PCE of 6.75%, demonstrating that the fluorination on D unit in D−A polymer is very promising and comparable to or even more effective than the fluorination on A unit for achieving high performance solar cells.[8b] Here one may have a question whether the photophysical properties and device performances can be further enhanced when both D and A units in the D−A type conjugated polymer are fluorinated. Recently, Hou et al.[6h] have achieved a high PCE of 8.6% with D−A polymer consisting of benzo[1,2-b:4,5-b']dithiophene and
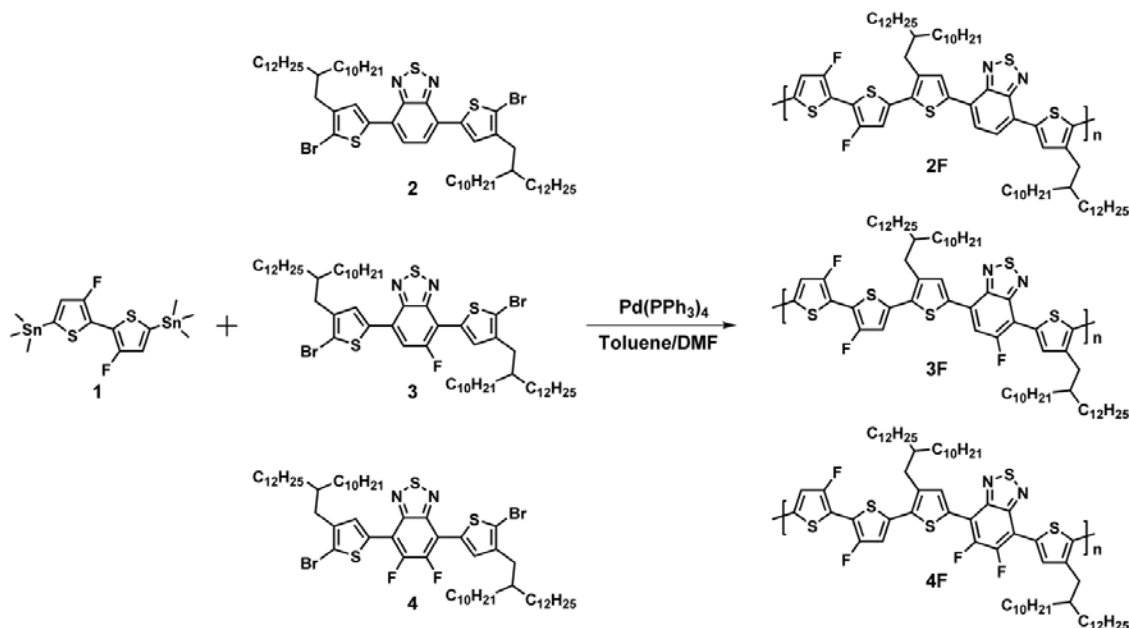
**Scheme 1** Synthesis of 2F, 3F and 4F polymers.

thieno[3,4-b]thiophene by fluorination on both D and A units for lowering molecular energy levels. However, to fully understand the effect of fluorination on both D and A units, more detailed studies based on polymers with different chemical structures should be required. In this work, we synthesized three fluorinated D–A polymers with different number of fluorination, consisting of 3,3'-difluoro-2,2'-bithiophene (D unit) and BT (A unit) with/without fluorination (Scheme 1), where the total number of fluorine atoms in polymer is controlled by the number of fluorine substitution on BT unit, in order to investigate the effect of the number of fluorine substitution on photophysical properties of polymers and their device performances of PSCs. We have observed that additional fluorine substitution on the A unit (BT) lowers further the frontier energy levels and enhances molecular ordering of the conjugated polymers, while two fluorine atoms are already introduced on the D unit. When compared with the polymer with non-fluorinated BT (denoted as 2F), the polymer with mono-fluorinated BT (denoted as 3F) shows higher PSC performances with a superior PCE of 9.14% but the polymer with di-fluorinated BT (denoted as 4F) exhibits a lower PCE of 6.43% because of higher bimolecular charge recombination and lower SCLC hole mobility. This result clearly demonstrates that the optoelectrical and photovoltaic properties of conjugated polymers are significantly affected by the number of fluorine atoms substituted on conjugated polymer, and therefore the number of fluorine substitution should be controlled for achieving high performance PSCs.

## Results and discussion

Three fluorinated polymers (2F, 3F and 4F) with different number of fluorine substitution were synthesized via the Stille coupling reaction in toluene/DMF with $Pd(PPh_3)_4$ as a catalyst, as shown in Scheme 1. Long and branched alkyl chains (2-decyltetradecyl) were introduced on conjugated backbone to ensure the solubility of fluorinated polymers in organic solvents. The number average molecular weights of 2F, 3F and 4F as measured by gel permeation chromatography (GPC) are 35, 33 and 40 kg $mol^{-1}$ with the

polydispersity index (PDI) of 1.60, 2.08 and 1.86, respectively (Table 1).

The effect of fluorine substitution on optical properties of the polymers is examined by UV–Vis spectroscopy (Figure 1). When the optical bandgaps of fluorinated polymers are determined from the onset of UV–Vis absorption spectra in film state and summarized in Table 1, it reveals that the bandgaps of 2F and 3F are nearly identical (1.57 eV) while 4F has a slightly wider bandgap of 1.59 eV. Notably, 3F and 4F polymers show stronger vibronic shoulder at around 705 nm than 2F polymer, indicating that the introduction of
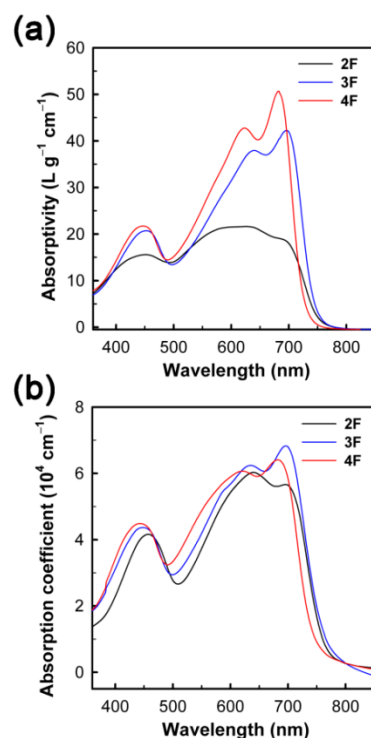


**Figure 1** UV–Vis absorption spectra of polymers in (a) $CHCl_3$ solution and (b) film state.

**Table 1** Characteristics of polymers.

| Polymer | $M_n$ [kg mol$^{-1}$] | PDI | $E_{g,opt}$[a] [eV] | Absorptivity at $\lambda_{max, solution}$ [L g$^{-1}$ cm$^{-1}$] | Absorption coefficient at $\lambda_{max, film}$ [10$^4$ cm$^{-1}$] | HOMO [eV] | LUMO[b] [eV] |
|---|---|---|---|---|---|---|---|
| 2F | 35 | 1.60 | 1.57 | 21.6 | 6.03 | −5.33 | −3.76 |
| 3F | 33 | 2.08 | 1.57 | 42.3 | 6.83 | −5.37 | −3.80 |
| 4F | 40 | 1.86 | 1.59 | 50.7 | 6.41 | −5.46 | −3.87 |

[a] Determined from the onset of UV−Vis absorption spectra.
[b] $E_{g,opt}$+HOMO.

fluorine atom on BT unit enhances interchain interaction between polymer chains.

Fluorine substitution on BT unit may also influence the electrochemical properties of polymers. Since strong electron-withdrawing ability of fluorine atom lowers the frontier energy levels of polymers, the HOMO energy level becomes deeper as the number of fluorine substitution increases: the HOMO energy levels of 2F, 3F and 4F are −5.33 eV, −5.37 eV and −5.46 eV, respectively (Figure S2 and Table 1). When the LUMO energy levels of polymers were estimated by adding the optical bandgap to the HOMO energy level, the 2F, 3F and 4F polymers have LUMO energy levels of −3.76, −3.80 and −3.87 eV, respectively, which provide sufficient LUMO level offset between polymer and PCBM (−4.3 eV) for effective exciton dissociation at the interface between donor and acceptor.[9]

The torsion angles in the backbone of fluorinated polymers are calculated by the density functional theory (DFT) with truncated molecular models (see Figure S3 and Table S1).[10] All fluorinated polymers exhibit nearly planar structure because the small size of fluorine atom does not significantly induce steric hindrance. This planarity of conjugated polymer backbone can improve intermolecular interaction between polymer chains and thus extend the π−conjugation. The DFT calculation also reveals that the HOMO and LUMO electrons in all fluorinated polymers are well localized on the D and A unit, respectively, indicating that the intramolecular charge transfer from D to A unit takes place effectively regardless of the number of fluorine substitution (Figure S3).

The charge-transport properties of polymers are measured by fabricating organic field-effect transistors (OFETs). The OFET performances are optimized at 150 °C annealing, and its device parameters are summarized in Table 2. Although all the polymers have low-lying energy levels due to strong electron-withdrawing ability of fluorine, all the devices exhibit typical behavior of *p*-channel transistor (Figure S4). The device with 4F exhibits the highest performance with a FET hole mobility of 0.62 cm$^2$ V$^{-1}$ s$^{-1}$, indicating that fluorination can improve the charge transport property of polymer. To compare the photovoltaic properties of

**Table 2** OFET characteristics of polymers annealed at 150 °C (channel width: 1 mm, length: 50 μm).

| Polymer | $\mu_h$ [cm$^2$ V$^{-1}$ s$^{-1}$] | $V_{th}$ [V] | $I_{on}/I_{off}$ |
|---|---|---|---|
| 2F | 0.33 | −7 | 10$^3$–10$^4$ |
| 3F | 0.37 | −10 | 10$^3$–10$^4$ |
| 4F | 0.62 | −5 | 10$^3$–10$^4$ |
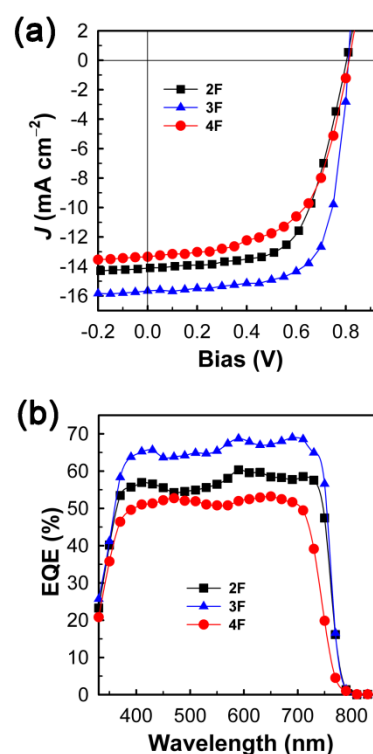


**Figure 2** (a) *J–V* curves and (b) EQE spectra of polymer:PC$_{71}$BM solar cells processed from DCB containing 2 vol% of CN in inverted device structure (ITO/ZnO/PEIE/ polymer:PC$_{71}$BM/MoO$_3$/Ag).

**Table 3** Photovoltaic properties of devices[a] fabricated from polymer:PC$_{71}$BM (1:1.5 w/w) blend processed from DCB containing 2 vol% of CN under standard AM 1.5G illumination

| Polymer | Thickness [nm] | $V_{OC}$ [V] | $J_{SC}$ [mA cm$^{-2}$] | FF [%] | PCE$_{max}$(ave) [%] |
|---|---|---|---|---|---|
| 2F | 115 | 0.80 | 14.1/13.8[b] | 63 | 7.11(6.76) |
| 3F | 130 | 0.82 | 15.7/15.4[b] | 71 | 9.14(8.79) |
| 4F | 120 | 0.82 | 13.3/13.4[b] | 59 | 6.43(6.15) |

[a]ITO/ZnO/PEIE/polymer:PC$_{71}$BM/MoO$_3$/Ag.
[b]Integrated from EQE data

fluorinated polymers, the PSCs were fabricated with an inverted device configuration of ITO/ZnO/polyethylenimine ethoxylated (PEIE)/polymer:PC$_{71}$BM/MoO$_3$/Ag.[11] The *J–V* characteristics of PSCs under AM 1.5G illumination are shown
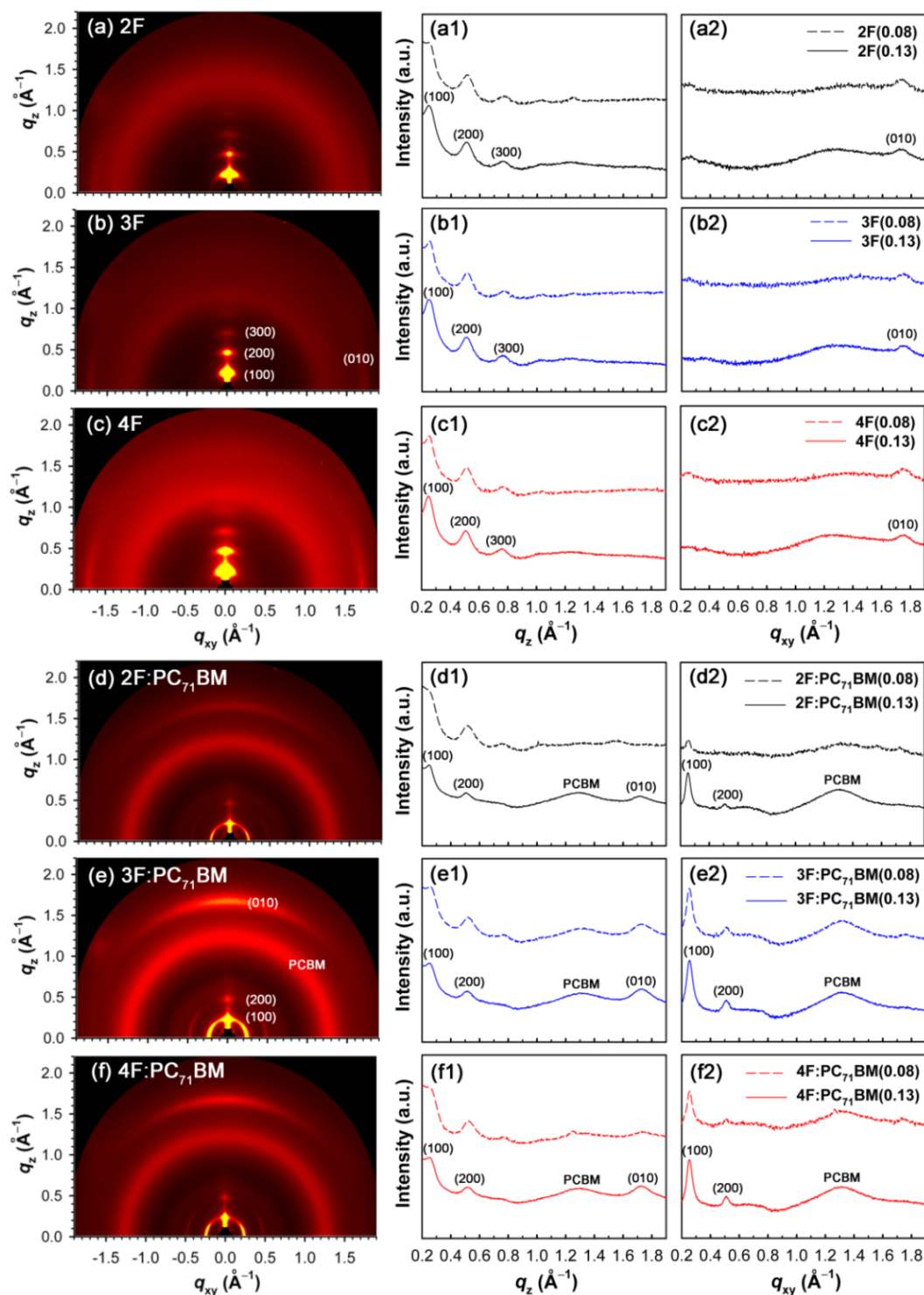
**Figure 3** GIWAXS images ($\alpha_i$ = 0.13°) of (a-c) pristine polymer films and (d-f) polymer:PC$_{71}$BM (1:1.5 w/w) blend films processed from DCB containing 2 vol% of CN; (middle column, a1-f1) $q_z$ and (right column, a2-f2) $q_{xy}$ scans of GIWAXS at two different incident angles ($\alpha_i$ = 0.08 and 0.13°) from (a1-c1 and a2-c2) pristine polymer films and (d1-f1 and d2-f2) polymer:PC$_{71}$BM(1:1.5 w/w) blend films processed from DCB containing 2 vol% of CN.

in Figure 2a and relevant photovoltaic properties are summarized in Table 3. The optimum blend ratio of polymer to PC$_{71}$BM was 1:1.5 when 2 vol% of 1-chloronaphthalene (CN) was used as an additive for the optimum morphology of active layer in PSCs.[12] Since the $V_{OC}$ of PSC is proportional to the difference between the HOMO energy level of donor polymer and the LUMO energy level of fullerene acceptor, the $V_{OC}$s of 3F and 4F are larger than 2F. Note here that the HOMO energy levels of 3F and 4F are deeper than 2F. While the 2F polymer exhibits a promising PCE of 7.11% with a $J_{SC}$ of 14.1 mA cm$^{-2}$, a $V_{OC}$ of 0.80 V and a FF of 63%, the 3F polymer with mono-fluorinated BT unit exhibits much higher PCE of 9.14% with
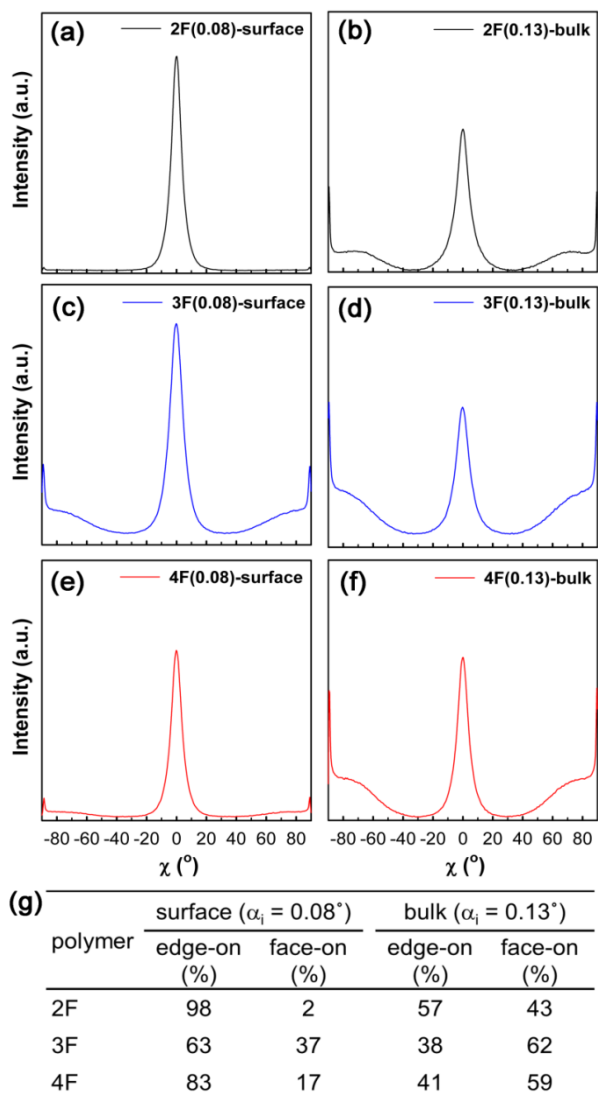
**Figure 4** Azimuthal angle scans of the (100) reflection from (a, b) 2F:PC$_{71}$BM, (c, d) 3F:PC$_{71}$BM and (e, f) 4F:PC$_{71}$BM blend films, which are processed from DCB containing 2 vol% of CN, at two incident angles of (a, c and e) $\alpha_i = 0.08$ and (b, d and f) $\alpha_I = 0.13°$; (g) the fractions of edge-on and face-on orientation of polymer crystals as calculated from the peak areas at $\chi = 0°$-45° (edge-on) and $\chi = 45°$-90° (face-on) in (a-f) azimuthal angle scans.

significantly enhanced $J_{SC}$ and FF ($J_{SC} = 15.7$ mA cm$^{-2}$, $V_{OC} = 0.82$ V and FF = 71%). However, the polymer with the di-fluorinated BT unit (4F) exhibits lower device performance with a PCE below 7%, demonstrating that the degree of fluorination on the conjugated polymer backbone should be controlled for achieving high efficiency. When the EQEs of devices were measured under monochromatic light, as shown in Figure 2b, it reveals that the 3F polymer exhibits higher EQE than 2F and 4F polymers in the entire range of wavelengths, consistent with higher $J_{SC}$ of solar cells with 3F.

For the purpose to investigate the reason why the 3F exhibits better photovoltaic performance than others, the bimolecular charge recombination in the active layer was estimated by measuring the photocurrent ($J_{ph}$) as a function of light intensity between 0.4 and 2 sun. When the photocurrent ($J_{ph}$) at $V = 0$ V is plotted against the
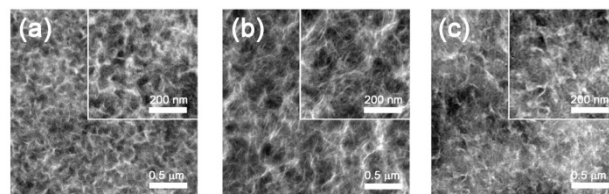
light intensity ($P_{light}$) in full logarithm scale, straight lines are obtained, as shown in Figure S5a. The relationship between $J_{ph}$ and $P_{light}$ can be represented by a power law equation: $J_{ph} \propto (P_{light})^\alpha$, where $\alpha$ is the recombination parameter and higher $\alpha$ value represents lower bimolecular recombination in the active layer.[13a,b,c] Since 2F:PC$_{71}$BM (0.97) and 3F:PC$_{71}$BM (0.98) shows higher $\alpha$ values than 4F:PC$_{71}$BM (0.95), the bimolecular recombination is more suppressed in the active layers with 2F and 3F polymers than the active layer with 4F polymer and this large bimolecular recombination loss in the active layer with 4F polymer may decrease $V_{OC}$s of solar cells with 4F.[13d,e]

The hole mobility in the active layer was also measured from dark $J-V$ curve of hole-only device by using the SCLC model (Figure S5b). Although the 4F polymer shows the highest FET hole mobility (Table 2), the SCLS hole mobility of the device with 3F:PC$_{71}$BM ($5.74 \times 10^{-4}$ cm$^2$ V$^{-1}$ s$^{-1}$) is higher than those of the devices with 2F:PC$_{71}$BM ($4.41 \times 10^{-4}$ cm$^2$ V$^{-1}$ s$^{-1}$) and 4F:PC$_{71}$BM ($2.75 \times 10^{-4}$ cm$^2$ V$^{-1}$ s$^{-1}$), implying that the charge carrier pathways are well developed in the active layer of PSC device fabricated from the 3F polymer. This will also be discussed in terms of the orientation of polymer crystals in the blend as follows.

Since the crystallinity and the crystal orientation of polymer are important parameters to determine the charge transport properties in photovoltaic device, the crystal properties of 2F, 3F and 4F polymers were investigated by the grazing incidence wide angle X-ray scattering (GIWAXS) with two different incident angles ($\alpha_i = 0.08$ and 0.13°) (Figure 3), where the X-ray with an incident angle of 0.08° ($\alpha_i \leq$ critical angle of the film) is sensitively diffracted on the near-surface region of the film and the X-ray with an incident angle of 0.13° (critical angle of the film $< \alpha_i <$ critical angle of the substrate) penetrates whole film thickness and thus provides the diffractions in the bulk of film.[14] In diffractions of all pristine films, only ($h00$) reflections are observed in the out-of-plane ($q_z$) direction, indicating that most of polymer crystals adopt the edge-on orientation on the substrate in the entire film thickness, and the intense (100) diffraction peaks at $q_z = 0.25$ Å$^{-1}$ corresponding to the interchain distance of 25.3 Å are observed for all polymers. The (010) diffraction peaks of pristine 2F, 3F and 4F polymer films are observed in-plane direction at $q_{xy} = 1.72$, 1.73 and 1.77 Å$^{-1}$, respectively, corresponding to the $\pi-\pi$ stacking distance of 3.66, 3.63 and 3.55 Å. The shorter $\pi-\pi$ stacking distance of 4F polymer may contribute to the higher FET hole mobility in OFET (Table 2). When the polymers are blended with PC$_{71}$BM, the crystal orientations of polymers are changed in blends. As shown in Figure 3(d1), 3(e1) and 3(f1), the diffractions of polymer:PC$_{71}$BM blend films as measured at an incident angle of 0.13° reveal that both (100) and (010) diffraction peaks are observed in out-of-plane direction, indicating that polymer crystals take both edge-on and face-on orientation (mixed orientation) in the bulk of blend films. However, when diffractions are measured at an incident angle of 0.08° for investigating the orientation of polymer crystals at the near-surface region of blend film, the 2F polymer crystals in the blend do not



**Figure 5** TEM images of (a) 2F:PC$_{71}$BM, (b) 3F:PC$_{71}$BM, and (c) 4F:PC$_{71}$BM blend films processed from DCB containing 2 vol% of CN.

show (010) diffraction in out-of-plane direction, implying that the edge-on orientation of 2F polymer crystals is dominant at the near surface region, while the 3F and 4F polymer crystals in the blend films still take mixed orientation with discernible (010) diffraction peaks in out-of-plane direction. The difference of crystal orientation between bulk and surface of blend films can be clearly seen in azimuthal angle scans of the (100) reflection (Figure 4). Since the intensity of peaks at near $\chi = 0°$ and near $\chi = \pm 90°$ are related to the edge-on and face-on orientation of crystallites, respectively,[14] the fractions of the edge-on and face-on orientations of polymer crystals can be directly calculated from the intensity ratio (Figure 4g). Another important feature is that the 3F polymer in blend has stronger tendency to take face-on orientation than other two polymers in both bulk and surface region of blend films, which contributes to higher SCLC hole mobility of 3F polymer in the active layer of PSC.

When the morphologies of three active layers as observed by transmission electron microscope (TEM) were compared, as shown in Figure 5, the 3F and 4F polymers in the blends form narrower fibrils than the 2F polymer, which is beneficial to exciton dissociation and charge generation, although all polymer blends develop interconnected network with nanoscale fibril structure. It has recently been reported that the fibril width is correlated to the solubility of polymer and that narrower fibrils are obtained by decreasing the solubility of polymer.[15a,b] Particularly, Liu et al.[15c] have shown that the size of phase separation in polymer:PCBM blend decreases with increasing the fluorine content of conjugated polymer. Hence, the reason for narrower fibril formation of 3F and 4F polymers in the blend is probably because more fluorine atoms in conjugated polymer decrease the solubility of polymers in organic solvent and thereby reduce the fibril size.

## Conclusions

We have presented the synthesis and photovoltaic properties of three fluorinated D–A polymers consisting of 3,3'-difluoro-2,2'-bithiophene and BT, where the fluorine content in the polymer is controlled by fluorination on BT unit. It has been observed that the introduction of fluorine atom causes multiple effects on the properties of conjugated polymers including stronger vibronic shoulder in UV–Vis absorption spectrum and lowering frontier energy levels. In particular, the crystal properties of fluorinated polymers are strongly dependent upon the total number of fluorine substitution in the polymer: the $\pi-\pi$ stacking distance decreases as the number of fluorine substitution on BT increases, affording the 4F polymer to the highest FET hole mobility, whereas the polymer (3F) with mono-fluorination on BT exhibits better photovoltaic performance than the polymers (2F and 4F) with non- and di-fluorination on BT, because the 3F polymer has stronger tendency to take face-on orientation than the 2F and 4F polymers when blended with PC$_{71}$BM, exhibiting the highest PCE of 9.14%. Our results have clearly demonstrated that the optoelectrical and photovoltaic properties of fluorinated conjugated polymers can be controlled by varying the amount of fluorine substituted on conjugated polymer backbone, and therefore the optimum amount of fluorine substitution should be considered for achieving high performance PSCs.

## Acknowledgements

## Notes and references

$^a$ Department of Materials Science and Engineering, Seoul National University, Gwanak-ro, Gwanak-gu, Seoul 151-744, Korea. E-mail: whjpoly@snu.ac.kr
$^b$ Pohang Accelerator Laboratory, Kyungbuk, Pohang 790-784, Republic of Korea.

1 (a) S. B. Darling, F. You, *RSC Adv.*, 2013, **3**, 17633; (b) C. L. Chochos, S. A. Choulis, *Prog. Polym. Sci.*, 2011, **36**, 1326; (c) A. J. Heeger, *Adv. Mater.*, 2014, **26**, 10.

2 (a) N. Blouin, A. Michaud, D. Gendron, S. Wakim, E. Blair, R. Neagu-Plesu, M. Belletete, G. Durocher, Y. Tao, M. Leclerc, *J. Am. Chem. Soc.*, 2008, **130**, 732; (b) H. X. Zhou, L. Q. Yang, S. C. Price, K. J. Knight, W. You, *Angew. Chem. Int. Ed.*, 2010, **49**, 7992; (c) J. H. Hou, H. Y. Chen, S. Q. Zhang, G. Li, Y. Yang, *J. Am. Chem. Soc.*, 2008, **130**, 16144; (d) C. H. Woo, P. M. Beaujuge, T. W. Holcombe, O. P. Lee, J. M. J. Fréchet, *J. Am. Chem. Soc.*, 2010, **132**, 15547; (e) J. W. Jo, S. S. Kim, W. H. Jo, *Org. Electron.*, 2012, **13**, 1322.

3 (a) Y.-C. Chen, C.-Y. Yu, Y.-L. Fan, L.-I. Hung, C.-P. Chen, C. Ting, *Chem. Commun.*, 2010, **46**, 6503; (b) Y.-X. Xu, C.-C. Chueh, H.-L. Yip, F.-Z. Ding, Y.-X. Li, C.-Z. Li, X. Li, W.-C. Chen, A. K.-Y. Jen, *Adv. Mater.*, 2012, **24**, 6356; (c) Y.-L. Chen, C.-Y. Chang, Y.-J. Cheng, C.-S. Hsu, *Chem. Mater.*, 2012, **24**, 3964; (d) I. Osaka, M. Shimawaki, H. Mori, I. Doi, E. Miyazaki, T. Koganezawa, K. Takimiya, *J. Am. Chem. Soc.*, 2012, **134**, 3498.

4 (a) L. Q. Yang, H. X. Zhou, W. You, *J. Phys. Chem. C*, 2010, **114**, 16793; b) C. Cabanetos, A. El Labban, J. A. Bartelt, J. D. Douglas, W. R. Mateker, J. M. J. Fréchet, M. D. McGehee, P. M. Beaujuge, *J. Am. Chem. Soc.*, 2013, **135**, 4656; (c) J. W. Jung, J. W. Jo, F. Liu, T. P. Russell, W. H. Jo, *Chem. Commun.*, 2012, **48**, 6933; (d) I. Osaka, M. Saito, T. Koganezawa, K. Takimiya, *Adv. Mater.*, 2014, **26**, 331; (e) S. Subramaniyan, H. Xin, F. S. Kim, S. Shoaee, J. R. Durrant, S. A. Jenekhe, *Adv. Energy Mater.*, 2011, **1**, 854; (f) Y. Li, *Acc Chem. Res.*, 2012, **45**, 723; (g) Z.-G. Z, Y. Li, *Sci. China Chem.*, 2015, **58**, 192.

5 (a) J. K. Park, J. Jo, J. H. Seo, J. S. Moon, Y. D. Park, K. Lee, A. J. Heeger, G. C. Bazan, *Adv. Mater.*, 2011, **23**, 2430; (b) J. U. Lee, Y. D. Kim, J. W. Jo, J. P. Kim, W. H. Jo, *J. Mater. Chem.*, 2011, **21**, 17209.

6 (a) H. Y. Chen, J. H. Hou, S. Q. Zhang, Y. Y. Liang, G. W. Yang, Y. Yang, L. P. Yu, Y. Wu, G. Li, *Nat. Photonics*, 2009, **3**, 649; (b) H. X. Zhou, L. Q. Yang, A. C. Stuart, S. C. Price, S. B. Liu, W. You, *Angew. Chem. Int. Ed.*, 2011, **50**, 2995; (c) S. C. Price, A. C. Stuart, L. Q. Yang, H. X. Zhou, W. You, *J. Am. Chem. Soc.*, 2011, **133**, 4625; (d) T. Okamoto, K. Nakahara, A. Saeki, S. Seki, J. H. Oh, H. B. Akkerman, Z. N. Bao, Y. Matsuo, *Chem. Mater.*, 2011, **23**, 1646; (e) C. Chang, L. Zuo, H. Yip, Y. Li, C. Li, C. Hsu, Y. Cheng, H. Chen, A. K.-Y. Jen, *Adv. Funct. Mater.*, 2013, **23**, 5084; (f) J. You, L. Dou, K. Yoshimura, T. Kato, K. Ohya, T. Moriarty, K. Emery, C.-C. Chen, J. Gao, G. Li, Y. Yang, *Nat. Commun.*, 2013, **4**, 1446; (g) T. L. Nguyen, H. Choi, S.-J. Ko, M. A. Uddin, B. Walker, S. Yum, J.-E. Jeong, M. H. Yun, T. J. Shin, S. Hwang, J. Y. Kim, H. Y. Woo, *Energy Environ. Sci.* 2014, **7**, 3040; (h) M. Zhang, X. Guo, S. Zhang, J. Hou, *Adv. Mater.*, 2014, **26**, 1118; (i) Y. Liu, J. Zhao, Z. Li, C. Mu,

W. Ma, H. Hu, K. Jiang, H. Lin, H. Ade, He. Yan, *Nat. Commun.*, 2014, **5**, 5293; (j) L. Ye, S. Zhang, W. Zhao, H. Yao, J. Hou, *Chem. Mater.*, 2014, **26**, 3603; (k) S. Zhang, L. Ye, W. Zhao, B. Yang, Q. Wang, J. Hou, *Sci. China Chem.*, 2015, **58**, 248.

7   (a) H. J. Son, W. Wang, T. Xu, Y. Liang, Y. Wu, G. Li, L. Yu, *J. Am. Chem. Soc.*, 2011, **133**, 1885; (b) W. Li, A. Furlan, W. S. C. Roelofs, K. H. Hendriks, G. W. P. van Pruissen, M. M. Wienk, R. A. J. Janssen, *Chem. Commun.*, 2014, **50**, 679; (c) J. H. Park, E. H. Jung, J. W. Jung, W. H. Jo, *Adv. Mater.*, 2013, **25**, 2583; (d) B. Carsten, J. M. Szarko, H. J. Son, W. Wang, L. Y. Lu, F. He, B. S. Rolczynski, S. J. Lou, L. X. Chen, L. P. Yu, *J. Am. Chem. Soc.*, 2011, **133**, 20468; (e) Y. Wang, X. Xin, Y. Lu, T. Xiao, X. Xu, N. Zhao, X. Hu, B. S. Ong, S. C. Ng, *Macromolecules*, 2013, **46**, 9587.

8   (a) J. W. Jo, J. W. Jung, H.-W. Wang, P. Kim, T. P. Russell, W. H. Jo, *Chem. Mater.*, 2014, **26**, 4214; (b) J. W. Jo, S. Bae, F. Liu, T. P. Russell, W. H. Jo. *Adv. Funct. Mater.*, 2015, **25**, 120.

9   C. J. Brabec, S. Gowrisanker, J. J. M. Halls, D. Laird, S. J. Jia, S. P. Williams, *Adv. Mater.*, 2010, **22**, 3839.

10 (a) S. B. Darling, *J. Phys. Chem. B*, 2008, **112**, 8891; (b) S. B. Darling, M. Sternberg, *J. Phys. Chem. B*, 2009, **113**, 6215; (c) R. S. Bhatta, M. Tsige, *Polymer*, 2014, **55**, 2667.

11 (a) S. Woo, W. H. Kim, H. Kim, Y. Yi, H.-K. Lyu, Y. Kim, *Adv. Energy Mater.*, 2014, **4**, 1301692; (b) Y. Zhou, C. Fuentes-Hernandez, J. Shim, J. Meyer, A. J. Giordano, H. Li, P. Winget, T. Papadopoulos, H. Cheun, J. Kim, M. Fenoll, A. Dindar, W. Haske, E. Najafabadi, T. M. Khan, H. Sojoudi, S. Barlow, S. Graham, J.-L. Brédas, S. R. Marder, A. Kahn, B. Kippelen, *Science*, 2012, **336**, 327.

12 (a) J. S. Moon, C. J. Takacs, S. Cho, R. C. Coffin, H. Kim, G. C. Bazan, A. J. Heeger, *Nano Lett.*, 2010, **10**, 4005; (b) Z. Chen, P. Cai, J. Chen, X. Liu, L. Zhang, L. Lan, J. Peng, Y. Ma, Y. Cao, *Adv. Mater.*, 2014, **26**, 2586. (c) X. Guo, C. Cui, M. Zhang, L. Huo, Y. Huang, J. Hou, Y. Li, *Energy Environ. Sci.* 2012, **5**, 7943.

13 (a) S. R. Cowan, A. Roy, A. J. Heeger, *Phys. Rev. B*, 2010, **82**, 245207; (b) S. R. Cowan, J. Wang, J. Yi, Y. J. Lee, D. C. Olson, J. W. P. Hsu, *J. Appl. Phys.*, 2013, **113**, 154504; (c) A. C. Stuart, J. R. Tumbleston, H. Zhou, W. Li, S. Liu, H. Ade, W. You, *J. Am. Chem. Soc.*, 2013, **135**, 1806; (d) M. D. Perez, C. Borek, S. R. Forrest, M. E. Thompson, *J. Am. Chem. Soc.*, 2009, **131**, 9281; (e) A. Maurano, R. Hamilton, C. G. Shuttle, A. M. Ballantyne, J. Nelson, B. O'Regan, W. Zhang, I. McCulloch, H. Azimi, M. Morana, C. J. Brabec, J. R. Durrant, *Adv. Mater.*, 2010, **22**, 4987.

14 (a) G. Kim, S.-J. Kang, G. K. Dutta, Y.-K. Han, T. J. Shin, Y.-Y. Noh, C. Yang, *J. Am. Chem. Soc.*, 2014, **136**, 9477; (b) J. Rivnay, R. Steyrleuthner, L. H. Jimison, A. Casadei, Z. Chen, M. F. Toney, A. Facchetti, D. Neher, A. Salleo, *Macromolecules*, 2011, **44**, 5246; (c) X. Zhang, H. Bronstein, A. J. Kronemeijer, J. Smith, Y. Kim, R. J. Kline, L. J. Richter, T. D. Anthopoulos, H. Sirringhaus, K. Song, M. Heeney, W. Zhang, I. McCulloch, D. M. DeLongchamp, *Nat. Commun.*, 2013, **4**, 2238; (d) S. Himmelberger, J. Dacuña, J. Rivnay, L. H. Jimison, T. McCarthy-Ward, M. Heeney, I. McCulloch, M. F. Toney, A. Salleo, *Adv. Funct. Mater.*, 2013, **23**, 2091; (e) W. Chen, M. P. Nikiforov, S. B. Darling, *Energy Environ. Sci.* 2012, **5**, 8045.

15 (a) W. Li, K. H. Hendriks, A. Furlan, W. S. C. Roelofs, M. M. Wienk, R. A. J. Janssen, *J. Am. Chem. Soc.*, 2013, **135**, 18942; (b) W. Li, K. H. Hendriks, A. Furlan, W. S. Roelofs, S. C. Meskers, M. M. Wienk, R. A. J. Janssen, *Adv. Mater.*, 2014, **26**, 1565; (c) P. Liu, K. Zhang, F.

Liu, Y. Jin, S. Liu, T. P. Russell, H.- L. Yip, F. Huang, Y. Cao, *Chem. Mater.*, 2014, **26**, 3009.

## Table of Contents

Three fluorinated D–A polymers, consisting of 3,3'-difluoro-2,2'-bithiophene and 2,1,3-benzothiadiazole with different number of fluorine substitution, are synthesized. The polymer with mono-fluorinated 2,1,3-benzothiadiazole exhibits a superior power conversion efficiency of 9.14%.
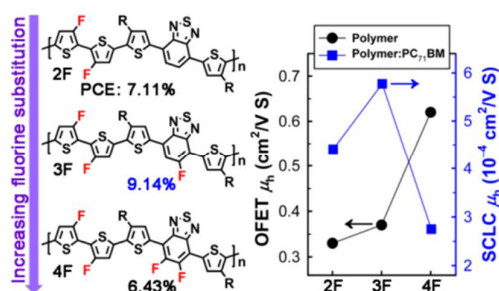


**TOC figure**

## Broader Context

Development of new semi-conducting polymers plays a critical role to improve the power conversion efficiency (PCE) of polymer solar cells (PSCs). Among various approaches to develop high performance conjugated polymers, the introduction of fluorine atom on alternating conjugated copolymer composed of electron-donating (D) and electron-accepting (A) units has recently been considered as a promising approach because of its unique advantages including energy level lowering without sacrifice of bandgap and improvement of molecular ordering by induced dipole along C–F bond, and no steric hindrance due to small size of fluorine atom. However, the fluorination can also lead to negative effects on polymer properties such as low solubility in organic solvent, unsuitable energy level for exciton separation and charge transport, and large aggregation of polymer chains in the active layer of PSCs. Hence, the degree of fluorination should be optimized to achieve high efficiency of PSCs. In this work, we synthesized three fluorinated polymers, consisting of 3,3'-difluoro-2,2'-bithiophene and 2,1,3-benzothiadiazole (BT) with different number of fluorine substitution, and their optoelectrical, photophysical and photovoltaic properties are compared to find the optimum fluorination. Among the three fluorinated polymers, the polymer with mono-fluorinated BT has outstanding device performance with a superior PCE of 9.14%.